

# Using light to study boundary lubrication: spectroscopic study of confined fluids

BY SUNG CHUL BAE<sup>1</sup>, JANET S. WONG<sup>1</sup>, MINSU KIM<sup>3</sup>, SHAN JIANG<sup>1</sup>,  
LIANG HONG<sup>1</sup> AND STEVE GRANICK<sup>1,2,3,\*</sup>

<sup>1</sup>*Department of Materials Science and Engineering*, <sup>2</sup>*Department of Chemistry*,  
and <sup>3</sup>*Department of Physics, University of Illinois at Urbana Champaign,*  
*Urbana, IL 61801, USA*

Several instrumental developments to examine the spectroscopic response of molecularly thin fluids confined between mica sheets are described. They are predicated on using a redesigned surface forces apparatus where dielectric coatings, transparent to light at needed optical wavelengths, retain the ability to measure interferometric thickness at other optical wavelengths. Examples of recent measurements are presented using confocal laser Raman spectroscopy to evaluate how molecules orient as well as to perform chemical imaging. Other examples are presented using confocal fluorescence recovery after photobleaching to evaluate translational diffusion of confined polymer melts. The advantage of separating the mechanical average (force and friction) from direct information about structure and mobility at the molecular level is stressed.

**Keywords:** fluorescence; Raman; confocal; spectroscopy; confined fluid

## 1. Introduction

Tribology and spectroscopy are traditionally regarded as distinct scientific disciplines. The molecular arrangements of how molecules in a tribological contact govern the transmission of friction forces between the confining solid surfaces, however, so it is natural that the field of nanotribology has evolved in directions to elucidate these questions also. Survey of the literature shows that computer simulations have provided the most direct information on this vital point, while on the experimental side, nanotribology experiments have focused on refining the available mechanics-based force information under ever-improved conditions of well-defined experimental conditions (Bhushan 2006).

The experimental study of nanotribology has been heavily influenced by the use of the surface forces apparatus (SFA), principally because the thickness between sliding solid surfaces can be so well defined when these surfaces are step-free, cleaved crystals of muscovite mica (Israelachvili 1991). Then, the thickness of the intervening film, usually a confined fluid film, can be resolved using optical

\* Author and address for correspondence: 104 S. Goodwin Avenue, Urbana, IL 61801, USA (sgranick@uiuc.edu).

One contribution of 8 to a Theme Issue ‘Nanotribology, nanomechanics and applications to nanotechnology I’.

interferometry with a resolution, depending on the care that is put into the experiment, that can be sub-angstrom. The initial experiments using mica (Bailey & Courtney-Pratt 1955; Tabor & Winterton 1969; Israelachvili & Adams 1978; Israelachvili *et al.* 1988; Van Alsten & Granick 1988) were later generalized in impressive new ways using atomic force microscopy (AFM) in the friction mode (Mate *et al.* 1987; Bhushan 2006), and also, more recently, related other devices (Bhushan 2006). However, a great limitation of all of the experiments performed in this spirit is that while they possess the attractive feature that the geometry of the sliding contact has been defined experimentally with unprecedented sharpness, even the most audacious and imaginative experiments of this kind give no direct information about how molecules are arranged. Force-based measurements, which inevitably are ensemble-averaged when so many molecules contribute to the overall force, can be interpreted at the molecular level only by the use of models.

Optics-based experiments can, in principle, overcome this limitation. This paper surveys experiments from this laboratory, using new experimental methods that we developed during the past 5 years, in which a variety of different spectroscopic experiments have been developed for use within the platform of the basic SFA—step-free single crystals of mica. Though the power of spectroscopic techniques in the studies of confined fluid has been of speculative interest for a long time, only a few successes have been reported so far. The laboratory of Safinya investigated the structure of thin smectic liquid crystal films under confinement using synchrotron X-ray scattering within the SFA (Golan *et al.* 2002). But it was not used to study ultrathin (of approx. nanometre-size) liquid films. Synchrotron waveguide methods were recently used to characterize the layering of molecularly thin films (Seeck *et al.* 2002). A microrheometer developed in this laboratory can readily be combined with spectroscopy (Fourier transform infrared spectroscopy and dielectric spectroscopy) or scattering (X-ray and neutron) techniques (Soga *et al.* 1998), and so also can a microrheometer developed in the laboratory of McKinley (Clasen *et al.* 2006). It uses two parallel optically flat window plates whose separation can be controlled from a few tens of nanometres to tens of micrometres, but is more suited for thicker (0.1–10  $\mu\text{m}$ ) films. By replacing one of the plates with a prism, recently it was shown that this rheometer can be combined with the surface-sensitive technique of infrared–visible sum-frequency generation (SFG) in the total internal reflection geometry (Mamedov *et al.* 2002). This combination can be used to probe the orientation, alignment and relaxation modes of organic molecules at the buried interface in a condition of flow or shear. A few years ago it was shown that SFG can also be combined with the SFA to study nanometre-thick films of one system of self-assembled monolayer confined between atomically smooth mica surfaces (Frantz *et al.* 1997), but implementation of this approach to other experimental situations has not been reported as yet.

## 2. Design requirements: challenges and solutions

### (a) *Dielectric coatings to go beyond the silver barrier*

The traditional methods of how to determine surface–surface separation and contact area, in a surface forces apparatus, employ a silver layer placed at the backside of the mica for this purpose. A severe limitation is that the high reflectivity of silver from the infrared to UV regime excludes optical experiments of the kind that we describe below.

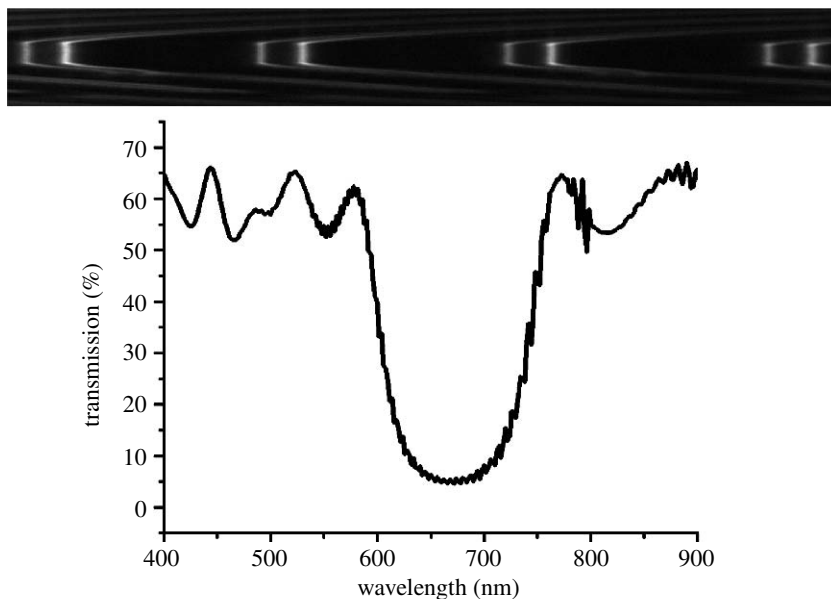


Figure 1. Transmission spectra of mica with nine alternate layers of  $\text{HfO}_x$  and  $\text{SiO}_x$  deposited to form a multilayer dielectric coating. High reflectivity in the region of approximately 680 nm allowed the use of traditional multiple-beam interferometry of incident white light to measure the surface–surface separation. The top inset illustrates the high quality of the resulting interference fringes (note that they appear as doublets, a ‘beta’ and a ‘gamma’ fringe, owing to mica’s birefringence). Excitation with the 488 nm line of an  $\text{Ar}^+$  laser allows one to perform single-photon fluorescence measurements and collect the fluorescence emitted at a higher wavelength than this. Excitation in the region near 800 nm with a Ti : sapphire laser allows one to perform two-photon fluorescence measurements. Excitation with a Nd : YAG laser (532 nm) and a He–Ne laser (633 nm) is also standard. By suitably varying the thickness of the layers of the optical coating, the regions of respective reflectivity and transmission are easily varied at will. The coating shown here was produced using electron-beam deposition in the Center for Microanalysis of Materials at the University of Illinois.

To remedy this, optical interferometry between silver coatings on the backside of the mica, used in the traditional surface forces apparatus, can be replaced by optical interferometry between multilayer dielectric coatings (Mukhopadhyay *et al.* 2002, 2003). We produced these multilayers by successive evaporation of multiple layers. In our original publication on this subject, 13 layers of  $\text{TiO}_x$  and  $\text{Al}_2\text{O}_3$  were grown by electron-beam evaporation (Mukhopadhyay *et al.* 2002) and the optical thickness of each layer was approximately  $\lambda/4$  ( $\lambda \sim 650$  nm), as determined by the optical monitor within the coating chamber. The desired thickness of each coating was calculated using software (J. A. Woolam Co., Inc., Lincoln, NE) so that the windows of reflectivity and translucency were controlled by the deposition conditions. This laboratory’s most recent experiments employ  $\text{HfO}_x$  and  $\text{SiO}_x$  instead due to a higher dielectric constant difference and nine alternate layers are found to suffice. With the most recent advance, the reflectivity as a function of wavelength can be measured.

In figure 1, transmission is plotted as a function of wavelength for a representative multilayer dielectric coating. One can see a region of high reflectivity—at these wavelengths, the surface–surface separation can be



Figure 2. A photograph of a redesigned surface forces apparatus mounted on the stage of an optical microscope. Compared with the traditional design, here the crossed mica cylinders are positioned 1–2 mm away from the microscope objective, allowing the use of microscope objectives with high NA and small working distance. In addition, thermal drift has been reduced by the symmetrical mechanical placement of the working elements in this design.

measured by traditional multiple-beam interferometry of incident white light. One can also see regions of high transmission—needed for fluorescence or Raman spectroscopy studies. It allows one to excite fluorescence through one spectral window, detect the induced fluorescence through a second spectral window and use multiple-beam interferometry to determine the film thickness at a third spectral window.

The adhesives traditionally used to attach mica sheets to a cylindrical lens cannot be used because they possess prohibitively large fluorescence. Instead, we often employ silicone elastomer (Sylgard 184, Dow Corning). In addition, when dealing with fluorescence experiments, to prolong the lifetime of the fluorophores, we use the lowest possible power (less than 1 mW for most applications) and the most stable dyes available commercially, although high laser power is sometimes needed for experiments involving Raman spectroscopy of confined films.

A photograph of this integrated platform for spectroscopy and mica force balance measurement is shown in figure 2. The mechanical placement of parts is more symmetric than in the traditional design—this reduces thermal drift. Even

more important, the mica sheets can be positioned within 1–2 mm of the microscope objective, thus allowing the experimenter to employ objectives of high numerical aperture (NA) and small working distance.

### 3. Spectroscopic findings

As force measurement carries no direct information regarding molecular composition, structure, conformation or mobility, we now turn to selected examples of how these varieties of information can be measured within the experimental platform described previously.

We begin with methods to measure structure and alignment. Fluorescence methods to study dynamics were introduced in earlier publications from this laboratory (Sukhishvili *et al.* 2000, 2002; Mukhopadhyay *et al.* 2002, 2003), as have infrared methods (Johnson & Granick 1992; Johnson *et al.* 1993; Frantz & Granick 1994; Schneider *et al.* 1996; Xie & Granick 2001). To measure structure and alignment, infrared spectroscopy was considered as a technique, but its implementation has been deferred for several reasons: first, owing to the difficulty of separating the molecularly thin absorption of interest from background absorption as the infrared beam traverses into and out of the experimental apparatus; and, second, owing to the interference fringes produced when a broadband infrared beam is directed at parallel mica sheets. A confocal geometry, using laser light to excite Raman signals, circumvents both difficulties.

#### (a) Chemical imaging of confined polymer chains

We have used confocal Raman spectroscopy to study how confinement alters the conformations of a polymer fluid, polydimethylsiloxane (PDMS), and also of a nematic liquid crystal, 4-cyano-biphenyl (6CB). Advantages of Raman spectroscopy include: (i) dye-free measurement, (ii) orientational information using polarized light, and (iii) chemical information from peak position and bandwidth analysis.

Figure 3*b* shows the Raman spectrum in the region of intense stretching vibrations of the methyl group. In the thinnest films studied, approximately 3–4 nm thick, the noise level was approximately 0.04 counts s<sup>-1</sup>, giving a signal-to-noise level of approximately 10. To measure Raman signals from films that are so thin, the usual approach of using the surface-enhanced Raman spectroscopy technique was not practical as it would have required the introduction of rough silver elements. We find that with signal acquisition times of 10–50 min, signals even from films so thin can be acquired using *unenanced* Raman scattering (Bae *et al.* 2005*a*).

By taking confocal Raman spectra at many positions, a contour map of the contact area was obtained (figure 3*a*). The peak intensity of the methyl group vibration was recorded for 1 min at spots spaced by 10 μm within the contact area and at spots spaced by 50 μm outside the contact area. By Beer's law, the intensity of the Raman signal was proportional to the thickness of the film; therefore, this comprised an image of the contact area. The diameter of the flattened contact, in this chemical image, agrees with the optical interferometry measurements that we also performed in parallel.

This illustrates the potential of chemical imaging of the contact area in a surface forces experiment (Bae *et al.* 2005*a*). In obvious ways, it can be extended to studies of phase separation (at rest and under shear), for example, as well as to

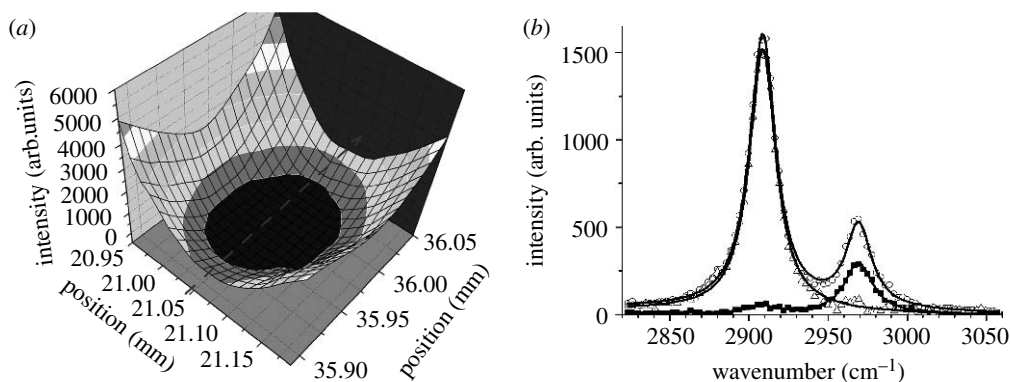


Figure 3. (a) Image of the contact spot acquired by recording the intensity of the methyl stretch vibration after confining the PDMS to a thickness of 3.5 nm, such that the mica sheets flattened at their apex to form parallel plates. Contours of equal relative intensity (arb. units) are denoted by different shadings. The film thickness of 3.5 nm is comparable to the thickness of a random coil of the narrow-distribution PDMS used, whose molecular weight was  $7060 \text{ g mol}^{-1}$ . This technique of chemical imaging contrasts with the optical interferometry that is used traditionally to image mica–mica contact. Adapted from Bae *et al.* (2005a). (b) Raman spectrum of PDMS, in the region of the methyl stretch (symmetric and asymmetric carbon–hydrogen stretch at  $2907$  and  $2965 \text{ cm}^{-1}$ , respectively). The polarized band (open circles), the depolarized band (filled squares) and the isotropic band (open triangles) are plotted separately.

studies of how shear orients fluid molecules. Using photoluminescence and absorption dichroism, this laboratory has reported studies in that direction (Bae *et al.* 2005b).

### (b) Orientation of a confined nematic liquid crystal

It is well known that a surface especially influences the nearby molecular arrangement of liquid crystals. In the case of liquid crystals, the surface ordering of molecules can extend far from the surface. Anisotropic friction due to molecular alignment has been reported in the bulk (de Gennes 1974) and for thin films (Artsyukhovich *et al.* 1999; Janik *et al.* 2001). Although the existence of some kind of complex interplay of the surface structure, molecular alignment and shear has been appreciated qualitatively for many years, this field still suffers from lack of quantitative understanding, mainly owing to the paucity of information at a level more direct than the force or friction response.

In the studies surveyed in §2 (Bae *et al.* 2005a), only two polarizations of a laser beam, parallel and perpendicular to the mica axes, were employed, due to the interfering birefringence of the mica sheets. In this section, we show the path towards obtaining complete information of molecular alignment; specifically, the order parameter and the alignment direction of a thin film, approximately 1 nm, confined between two single crystals of mica and how shear modifies them.

The liquid crystal was 4-cyano-4-hexylbiphenyl (6CB). It is in a crystalline phase below  $14.5^\circ\text{C}$ , a nematic phase between  $14.5$  and  $29.4^\circ\text{C}$  and isotropic above  $29.4^\circ\text{C}$ . The experiment was performed at a room temperature of  $25^\circ\text{C}$ . Many studies (Pieranski & Jérôme 1989; Jérôme & Shen 1993; Artsyukhovich *et al.* 1999;



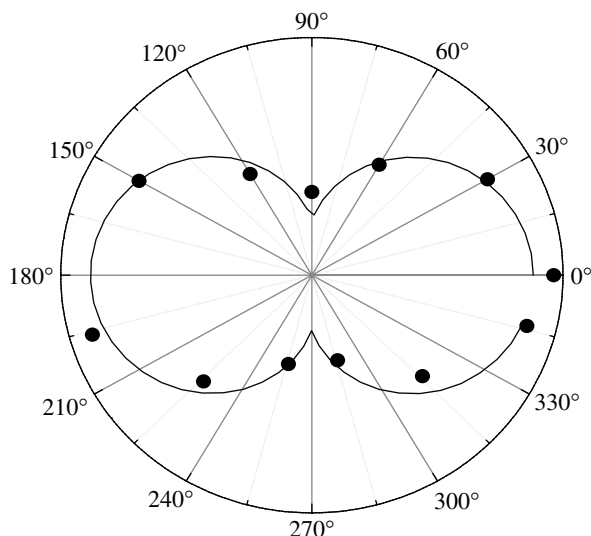


Figure 4. Polar plot of Raman intensity at different angles of linear laser polarization, for a film of 6CB confined to a thickness of 1 nm between crystallographically ordered mica sheets. From data of this kind, the order parameter is deduced as described in the text.

Kitaev & Kumacheva 2000) have shown that cyanobiphenyls are anchored at  $30^\circ$  from the  $\gamma$ -optical axis of mica anticlockwise and clockwise alternatively for adjacent layers of mica. A separate AFM study indicated that mica is grooved at the angle of  $30^\circ$  from the  $\gamma$ -optical axis (Kuwahara 1999) and that molecules are expected to sit along the groove. After 6CB was confined to the thickness of 1 nm, the Raman intensity of its biphenyl ring was obtained at different angles of the linear laser polarization. Two strong peaks of the biphenyl ring vibration and nitrile (CN) vibration appear at  $1610$  and  $2230\text{ cm}^{-1}$ , respectively. When the analysis of these two peaks was performed, they showed the same trend of change, and considering their modes of vibration (if a plane of the ring is parallel to a mica surface, intensities of the Raman peaks at different angles should be the same due to symmetry), this can be only explained when the rings in 6CB are standing almost perpendicular (there is a torsion angle of  $46^\circ$  between two planes of rings) to a plane of mica. This agrees well with an X-ray study of cyanobiphenyls (Leadbetter & Mehta 1981).

This gives polar plots of the kind illustrated in figure 4. For analysis, the data are described as  $I(\theta) = a \times \cos^2(\theta + \theta_0) + b$  and the ratio  $a/b$  defines the order parameter, while the angle  $\theta_0$  defines the mean angle of molecular alignment. Furthermore, detailed considerations show that the error owing to mica birefringence is negligible, of the order of 0.1% for mica sheets  $5\text{ }\mu\text{m}$  thick. The frequency of oscillatory shear was kept at 1.3 Hz for all sets of experiments while the amplitude of shear was varied.

To explore the effect of shear, oscillatory shear was applied at 1.3 Hz while the amplitude of shear was varied. First, grooves of two sheets of mica were aligned parallel to the shear direction. The decrease in the order parameter compared with the bulk order parameter was due to unavoidable slight mismatch of two mica grooves. Figure 5a shows that when small displacement of shear was

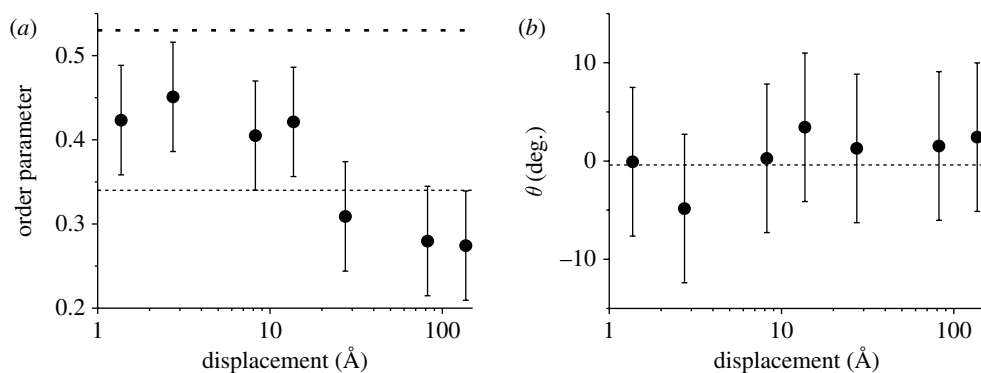


Figure 5. Influence of shear on (a) order parameter and (b) alignment angle of 6CB confined between crystallographically aligned mica sheets (grooves parallel) and sheared parallel to the groove. The order parameter and alignment angle were determined by the method summarized in the text. (a) Dotted and dashed lines represent the order parameter at the bulk and at rest (no shear), respectively. (b) Dashed line is the average of all points.

applied, molecules aligned better as indicated by the increase in the order parameter, but that displacements above 1 nm in amplitude caused it to revert back to the value without shear or less than that.

Figure 5b shows that the absolute values of the alignment angles were unaffected by shear, even though the perfection of alignment was affected. Under current exploration in this laboratory is how the alignment of a confined liquid crystal is influenced by two competing crystal structures of upper and lower mica sheets (the relative crystallographic orientation of the two mica sheets), and also the question of how ordering is modified by the angle of shear relative to the mica axes.

### (c) Surface diffusion of confined polymer chains

The diffusion of polymer chains at solid surfaces is crucial in determining properties as diverse as fracture properties of polymer composites, polymer surface glass transition, biocompatible coatings, friction and lubrication, and adhesion. Yet the understanding of this area is rather limited. While simulations have been performed, there exist no direct measurements to contrast polymer melt diffusion in molecularly thin films with the friction that has so often been measured.

This is basically due to the lack of proper experimental tools and the large number of variables involved. The experimentation on examining the dynamics of confined polymers is difficult because, first, the confinement has to be well defined if any meaningful mechanical parameters are to be extracted. Second, the technique should allow independent control of experimental parameters such as film thickness, surface wettability and shear deformation, so that potential contributing factors can be separated. Third, the polymer dynamics is expected to be very slow when it is under confinement. Polymer diffusion is usually too slow to evaluate using the methods of fluorescence correlation spectroscopy (FCS) previously employed by this laboratory (Sukhishvili *et al.* 2000, 2002; Mukhopadhyay *et al.* 2002, 2003). Others previously used fluorescence recovery



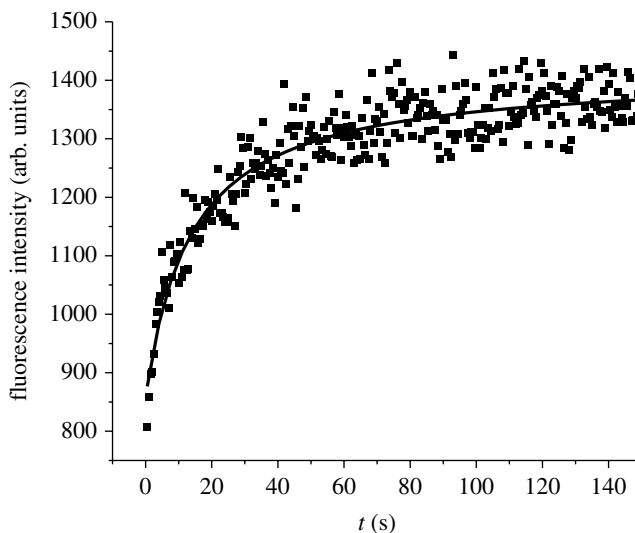


Figure 6. FRAP for narrow-distribution Bodipy-labelled PDMS with number-average molecular weight of  $2400 \text{ g mol}^{-1}$ . This polymer was squeezed between crystallographically oriented mica sheets to a thickness of  $1.8 \text{ nm}$  and, before measurements, 12 hours were allowed for equilibration, as discussed in the text. The mica sheets were cleaved using the method of tape cleaving described elsewhere (Zhu & Granick 2003).

after photobleaching (FRAP) to measure chain mobility in thin (unconfined) solid films (Frank *et al.* 1996).

For the FRAP measurements presented below, fluorescent probes in a given area are first photobleached using laser light of high intensity, then the inflow of unbleached molecules is monitored using light of lower intensity. The diffusion coefficient is calculated by fitting the fluorescence recovered over time to the diffusion equation.

In preliminary experiments using Bodipy-FL-labelled low-molecular-weight PDMS, figure 6 presents fluorescence recovery curves for a film  $1.8 \text{ nm}$  thick. First, the fluorescence within a spot of approximately  $0.3 \mu\text{m}$  in diameter was bleached using an intense but short pulse from the  $488 \text{ nm}$  line of an  $\text{Ar}^+$  laser, then the intensity of the bleached area was monitored with a much weaker probe beam. A single exponential time constant described the fluorescence recovery curves very well. Nanorheology experiments show that the shear viscosity of confined PDMS melts starts to rise above that of the bulk at the distance of approximately  $5\text{--}6 R_g$  (Van Alsten & Granick 1990; Granick & Hu 1994), which, for the molecular weight of PDMS used here (see figure 6 legend), is approximately  $10 \text{ nm}$ .

For the data in figure 6, the thickness of the film is  $1.8 \text{ nm}$  and the implied diffusion coefficient is  $D \approx 1 \times 10^{-13} \text{ m}^2 \text{ s}^{-1}$ , one-third of that obtained from unconfined PDMS surface diffusion. The observed reduction in diffusion coefficient (figure 6) might also be influenced by adsorption from the melt to mica. In extending these preliminary data, which present a proof of concept, experiments to explore the thickness dependence as well as dependence on chain length are ongoing.

#### 4. Prospects

This survey of instrumental developments for the study of confined fluids between single crystals of mica, based on using methods of fluorescence and vibrational spectroscopy, presents methods designed to complement the ensemble-averaged, engineering-based, force measurements that presently dominate experimental work in this field. How do fluids organize when they are confined, in one or more directions, to less than the correlation length of short-range packing (Walley *et al.* 1994)? The natural disorder of the liquid state competes with the order induced by confining surfaces and the ‘friction’ differs from that expected from the viscosity of the parent, bulk fluid. This, the confined fluid problem, presents major intellectual challenges as well as significant practical ramifications, because molecularly thin fluids are ubiquitous in areas from tribology to geology. This explains why interest in confined fluids is so intense.

However, a survey of the literature shows that most of what is known about how the transport properties of molecularly thin fluids vary with thickness depends on measuring forces, especially the surface forces and friction of fluids confined between atomically smooth sheets of muscovite mica. Thus, experiments on this question were based mainly on macroscopic force measurements, leaving open the question of what actually happens at the molecular level.

How does the mechanical property, friction, relate to how molecules orient? To diffusion? Otherwise stated: in this field that has hitherto been dominated by mechanical studies on the experimental side, what happens on the level of physical–chemical investigation? First, this will develop new understanding of how fluids assemble and diffuse in molecularly thin confined geometries. This is fundamental in many scientific and technical applications, including friction, adhesion, geology and the mechanical behaviour of composite and nanocomposite materials.

It is the laboratory’s hope that the Raman spectroscopy and fluorescence methods sketched here may find general application in other research groups, as the equipment needed to duplicate the experimental platforms illustrated here would be relatively straightforward now that the experimental protocols have been developed.

In a larger sense, the time is right to address squarely the microscopic motions, relaxations and structural rearrangements of molecules in confined geometries. In the long run, this research seeks to map connections between the macroscopic observables (friction, adhesion and various other forces) and the molecular parameters that give rise to them. A long-term goal in this field of study is that friction and adhesion arising from molecularly thin films at surfaces should become as well understood as molecular conformations already are in the bulk. To achieve this, and to stimulate theoretical interest in the problem, quantitative data are needed on how surface conformations and diffusion depend on normal load, position within a squeezed contact zone and film thickness.

This study was supported by the National Science Foundation under grant NSF-CMS-0555820. For partial support, we acknowledge grants NSF-DMR-0605947, NSF-DMR-0117792 and NSF (NIRT) CBET 060978, and the US Department of Energy, Division of Materials Science, under award no. DEFG02-02ER46019.

## References

- Artsyukhovich, A., Broekman, L. D. & Salmeron, M. 1999 Friction of the smectic-A liquid crystal (8CB) as probed by surface forces apparatus. *Langmuir* **15**, 2217–2223. (doi:10.1021/la980415m)
- Bae, S. C., Lee, H., Lin, Z. & Granick, S. 2005a Chemical imaging in a surface forces apparatus: confocal Raman spectroscopy of confined PDMS. *Langmuir* **13**, 5685–5688. (doi:10.1021/la050233+)
- Bae, S. C., Lin, Z. & Granick, S. 2005b Conjugated polymers confined and sheared: photoluminescence and absorption dichroism in a surface forces apparatus. *Macromolecules* **38**, 9275–9279. (doi:10.1021/ma0510035)
- Bailey, A. I. & Courtney-Pratt, J. S. 1955 The area of real contact and the shear strength of monomolecular layers of a boundary lubricant. *Proc. R. Soc. A* **227**, 500–515. (doi:10.1098/rspa.1955.0026)
- Bhushan, B. (ed.) 2006 *Springer handbook of tribology*, 2nd edn. New York, NY: Springer.
- Clasen, C., Georing, B. P. & McKinley, G. H. 2006 The flexure-based microgap rheometer (FMR). *J. Rheol.* **50**, 883–905. (doi:10.1122/1.2357190)
- de Gennes, P.-G. 1974 *The physics of liquid crystals*. Oxford, UK: Oxford University Press.
- Frank, B., Gast, A. P., Russell, T. P., Brown, H. R. & Hawker, C. 1996 Polymer mobility in thin films. *Macromolecules* **29**, 6531–6534. (doi:10.1021/ma960749n)
- Frantz, P. & Granick, S. 1994 Exchange kinetics of adsorbed polymer and the achievement of conformational equilibrium. *Macromolecules* **27**, 2553–2558. (doi:10.1021/ma00087a025)
- Frantz, P., Wolf, F., Xiao, X.-d., Chen, Y., Bosch, S. & Salmeron, M. 1997 Design of a surface forces apparatus for tribology studies combined with non-linear optical spectroscopy. *Rev. Sci. Instrum.* **68**, 2499–2504. (doi:10.1063/1.1148148)
- Golan, Y., Seitz, M., Luo, C., Martin-Herranz, A., Yasa, M., Li, Y., Safinya, C. R. & Israelachvili, J. 2002 The X-ray surface forces apparatus for simultaneous X-ray diffraction and direct normal and lateral force measurements. *Rev. Sci. Instrum.* **73**, 2486–2488. (doi:10.1063/1.1480461)
- Granick, S. & Hu, H.-W. 1994 Nanorheology of confined polymer melts, 1. Linear shear response at strongly absorbing surfaces. *Langmuir* **10**, 3857–3866. (doi:10.1021/la00022a076)
- Israelachvili, J. N. 1991 *Intermolecular and surface forces*, 2nd edn. New York, NY: Academic Press.
- Israelachvili, J. N. & Adams, G. E. 1978 Measurement of forces between two mica surfaces in aqueous electrolyte solutions in the range 0–100 nm. *J. Chem. Soc. Farad. Trans. I* **74**, 975–1001. (doi:10.1039/f19787400975)
- Israelachvili, J. N., McGuiggan, P. M. & Homola, A. M. 1988 Dynamic properties of molecularly thin liquid films. *Science* **240**, 189–191. (doi:10.1126/science.240.4849.189)
- Janik, J., Tadmor, R. & Klein, J. 2001 Shear of molecularly confined liquid crystals II: stress anisotropy across a model nematogen compressed between sliding solid surfaces. *Langmuir* **17**, 5476–5485. (doi:10.1021/la001392q)
- Jérôme, B. & Shen, Y. R. 1993 Anchoring of nematic liquid crystals on mica in the presence of volatile molecules. *Phys. Rev. E* **48**, 4556–4574. (doi:10.1103/PhysRevE.48.4556)
- Johnson, H. E. & Granick, S. 1992 New mechanism of nonequilibrium polymer adsorption. *Science* **255**, 966–968. (doi:10.1126/science.255.5047.966)
- Johnson, H. E., Douglas, J. F. & Granick, S. 1993 Topological influences on polymer adsorption and desorption dynamics. *Phys. Rev. Lett.* **70**, 3267–3270. (doi:10.1103/PhysRevLett.70.3267)
- Kitaev, V. & Kumacheva, E. 2000 Thin films of liquid crystals confined between crystalline surfaces. *Phys. Chem. B* **104**, 8822–8829. (doi:10.1021/jp992996+)
- Kuwahara, Y. 1999 Muscovite surface structure imaged by fluid contact mode AFM. *Phys. Chem. Miner.* **26**, 198–205. (doi:10.1007/s002690050177)
- Leadbetter, A. J. & Mehta, A. I. 1981 Molecular packing in the nematic phase of cyano compounds with different ring systems. *Mol. Cryst. Liquid Cryst.* **72**, 51–57. (doi:10.1080/01406568108084036)

- Mamedov, S., Schwab, A. D. & Dhinojwala, A. 2002 A device for surface study of confined micron thin films in a total internal reflection geometry. *Rev. Sci. Instrum.* **73**, 2321–2324. (doi:10.1063/1.1473222)
- Mate, C. M., McClelland, G. M., Erlandsson, R. & Chiang, S. 1987 Atomic-scale friction of a tungsten tip on a graphite surface. *Phys. Rev. Lett.* **59**, 1942–1945. (doi:10.1103/PhysRevLett.59.1942)
- Mukhopadhyay, A., Zhao, J., Bae, S. C. & Granick, S. 2002 Contrasting friction and diffusion in molecularly thin confined films. *Phys. Rev. Lett.* **89**, 136 103. (doi:10.1103/PhysRevLett.89.136103)
- Mukhopadhyay, A., Zhao, J., Bae, S. C. & Granick, S. 2003 An integrated platform for surface forces measurements and fluorescence correlation spectroscopy. *Rev. Sci. Instrum.* **74**, 3067. (doi:10.1063/1.1570947)
- Pieranski, P. & Jérôme, B. 1989 Adsorption-induced anchoring transitions at nematic-liquid-crystal-crystal interfaces. *Phys. Rev. A* **40**, 317–322. (doi:10.1103/PhysRevA.40.317)
- Schneider, H. M., Frantz, P. & Granick, S. 1996 The bimodal energy landscape when polymers adsorb. *Langmuir* **12**, 994–996. (doi:10.1021/la950556d)
- Seeck, O. H., Kim, H., Lee, D. R., Shu, D., Kaendler, I. D., Basu, J. K. & Sinha, S. K. 2002 Observation of thickness quantization in liquid films confined to molecular dimension. *Europhys. Lett.* **60**, 376–382. (doi:10.1209/epl/i2002-00274-6)
- Soga, I., Dhinojwala, A. & Granick, S. 1998 Opto-rheological studies of sheared confined fluids with mesoscopic thickness. *Langmuir* **14**, 1156–1161. (doi:10.1021/la970812h)
- Sukhishvili, S. A., Chen, Y., Müller, J. D., Schweizer, K. S., Gratton, E. & Granick, S. 2000 Diffusion of a polymer ‘Pancake’. *Nature* **406**, 146. (doi:10.1038/35018166)
- Sukhishvili, S. A., Chen, Y., Müller, J. D., Gratton, E., Schweizer, K. S. & Granick, S. 2002 Surface diffusion of poly(ethylene glycol). *Macromolecules* **35**, 1776–1784. (doi:10.1021/ma0113529)
- Tabor, D. & Winterton, R. H. S. 1969 The direct measurement of normal and retarded van der Waals forces. *Proc. R. Soc. A* **312**, 435–450. (doi:10.1098/rspa.1969.0169)
- Van Alsten, J. & Granick, S. 1988 Molecular tribometry of ultrathin liquid films. *Phys. Rev. Lett.* **61**, 2570–2573. (doi:10.1103/PhysRevLett.61.2570)
- Van Alsten, J. & Granick, S. 1990 Shear rheology in a confined geometry: polysiloxane melts. *Macromolecules* **23**, 4856–4862. (doi:10.1021/ma00224a014)
- Walley, K. P., Schweizer, K. S., Peanasky, J., Cai, L. & Granick, S. 1994 Structure of confined alkane liquids. *J. Chem. Phys.* **100**, 3361–3364. (doi:10.1063/1.466377)
- Xie, A. F. & Granick, S. 2001 Weak versus strong: a weak polyacid embedded within a multilayer of strong polyelectrolytes. *J. Am. Chem. Soc.* **123**, 3175–3176. (doi:10.1021/ja005818z)
- Zhu, Y. & Granick, S. 2003 Reassessment of solidification in fluids confined between mica sheets. *Langmuir* **19**, 8148–8151. (doi:10.1021/la035155+)